

Dominant Reaction Mechanisms of Nucleon-Induced Particle Emission into the Continuum

A.A. Cowley^{1,2}

¹Department of Physics, Stellenbosch University, Private Bag X1, Matieland 7602, South Africa

²iThemba Laboratory for Accelerator Based Sciences, PO Box 722, Somerset West 7129, South Africa

Abstract. Results from various proton-induced two-proton coincidence studies are discussed. It is shown that a consistent interpretation emerges. Consequently a multistep interpretation of inclusive proton-induced reactions is explicitly shown to be valid.

1 Introduction

Inclusive reactions induced by nucleons at projectile energies in the range of 100 to hundreds of MeV have been the subject of extensive experimental and theoretical studies. At present a fairly consistent interpretation of the reaction mechanism is available, especially for the emission of nucleons. At the most basic level the interaction of a nucleon with an atomic nucleus at these incident energies should, due to the de Broglie wavelength of the projectile compared to the size of a bound nucleon, involve an initial NN collision in which the available kinetic is shared between the two colliding nucleons. However, the mean free path of these two intranuclear particles in nuclear matter is such that it is very likely that both will suffer further interactions with remaining nucleons in the target nucleus. These general ideas have been exploited and developed into successful theoretical formulations that are able to describe the so-called pre-equilibrium part of the emission spectrum accurately.

In this review I will discuss a progression of studies that start with examples of investigations of pure knockout of a nucleon from an atomic nucleus. This will be followed by experiments which were carefully designed to emphasise the further intranuclear rescattering of one of the participants in the initial NN collision. Finally the general multistep idea will be demonstrated to hold also for composite particle emission, and it will be shown that analyzing power measurements are very sensitive to the number of intranuclear steps before the final process that leads to emission of the ejectile. Although many investigations exist which would illustrate the effects that I point out equally well, or arguably

perhaps even better, I will restrict this review to results with which I have been personally involved.

2 Pre-Equilibrium Reactions

The dominant yield of nucleons from proton-induced nuclear reactions at incident energies of 100 to 200 MeV, is associated with pre-equilibrium [1] reactions. In terms of emission energy, this reaction process produces ejectiles at higher excitation energies of the residual nucleus than those at which discrete states of direct reactions are observed, but at energies above those of emission from a fully equilibrated system. The angular and energy distributions of these reactions are successfully described by a number of roughly equivalent quantum-mechanical formulations [2], of which the statistical multistep theory of Feshbach, Kerman and Koonin (FKK) [3] has been tested most often against experimental data. A typical example is shown in Figure 1. Contributions of the individual steps to the cross section as a function of scattering angle is displayed, and higher steps contribute progressively more at larger angles, and towards lower emission energy.

The pre-equilibrium cross section distributions are rather featureless, and in spite of the encouraging agreement between theoretical results and experimental

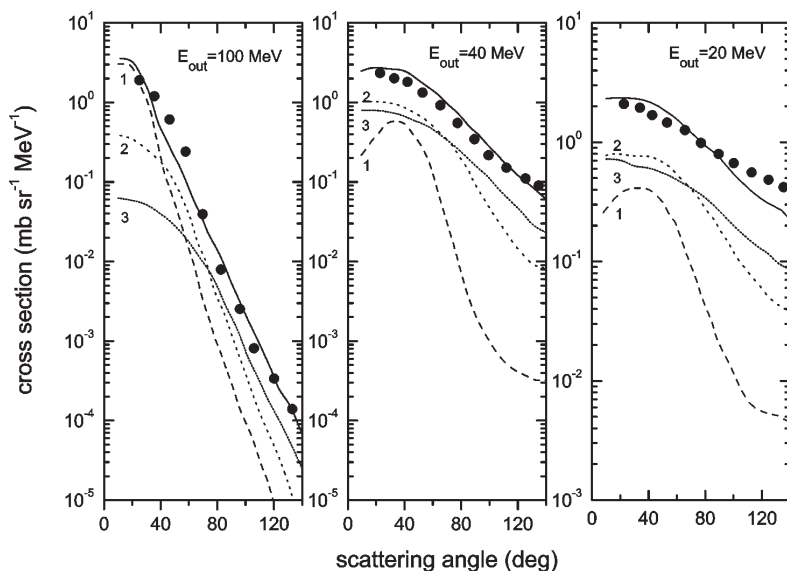


Figure 1. Pre-equilibrium cross section angular distributions for the inclusive reaction $^{90}\text{Zr}(p,p'x)$ at an incident energy of 120 MeV for emission energies as indicated. The curves are predictions of the FKK theory, with individual contributions from various multisteps as shown. Results are from Cowley *et al.* [4].

data, it would be desirable to obtain independent proof of the multistep nature of the reaction mechanism. In the subsequent sections a series of experiments will be discussed which investigate this aspect further.

3 Knockout Reactions of the $(p,2p)$ Type

The plane wave impulse approximation (PWIA) offers the most simplistic, and clearly unrealistic, viewpoint of a knockout reaction. Nevertheless, the cross section predicted by the PWIA provides a convenient yardstick against which the flux losses due to interactions of the projectile, and outgoing protons, with the spectator part of the target nucleus could be measured. In order to achieve this, a prediction of the distorted wave impulse approximation (DWIA) [5, 6] is required. Of course, this is only useful if the DWIA provides a good description of experimental data, an example of which is shown in Figure 2 (Results are from Ref. [7]). Figure 2 illustrates an energy-sharing distribution plotted as a function of the kinetic energy of one of the emitted protons from the $^{197}\text{Au}(p,2p)^{196}\text{Pt}$ reaction at an incident energy of 200 MeV. The data correspond to kinematic loci for knockout from valence orbitals of ^{197}Au . Clearly the DWIA gives an excellent reproduction of the shape of the distribution. Although the absolute mag-

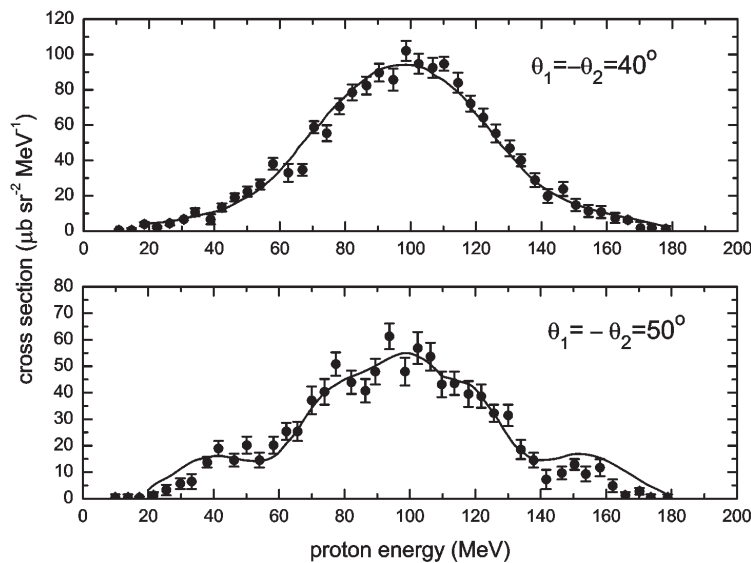


Figure 2. Energy sharing cross section distributions at an incident energy of 200 MeV for the reaction $^{197}\text{Au}(p,2p)^{196}\text{Pt}$ for knockout from unresolved valence orbitals of the target nucleus. Results are displayed as a function of the kinetic energy of one of the ejected protons. The curves represent predictions of the DWIA theory. Results are from Förtlisch *et al.* [7].

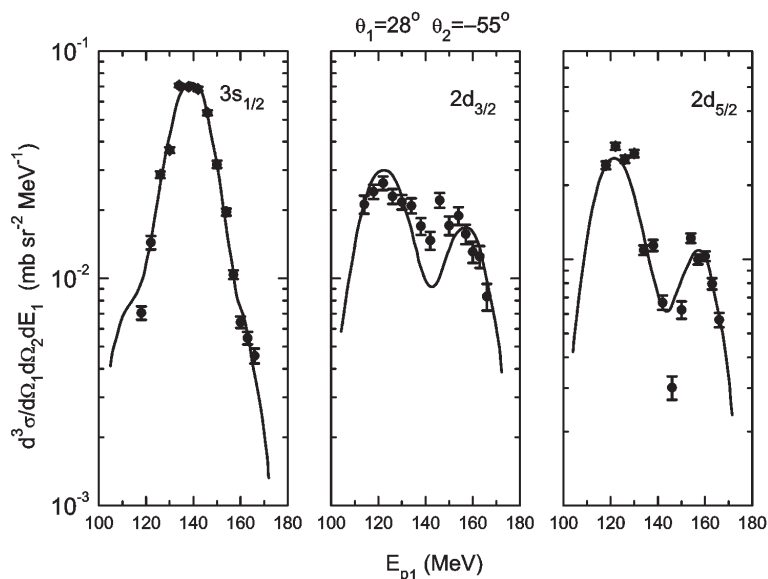


Figure 3. Energy sharing cross section distributions at an incident energy of 200 MeV for the reaction $^{208}\text{Pb}(p, 2p)^{207}\text{Tl}$ for knockout from the $3s_{1/2}$, $2d_{3/2}$ and $2d_{5/2}$ orbitals of the target nucleus. Results are displayed as a function of the kinetic energy of the proton observed at the angle indicated as θ_1 in the figure. The curves represent predictions of the DWIA theory. Results are from Neveling *et al.* [8].

nitude of the theory is based on normalization to the data, the extracted number appears to be reasonable. In fact, this number can be evaluated by comparing results for $^{208}\text{Pb}(p, 2p)^{207}\text{Tl}$ at an incident energy of 200 MeV (see Figure 3) with $(e, e'p)$ studies, as well as with theoretical estimates. Consistent results are obtained, with a spectroscopic value for knockout of $3s_{1/2}$ protons (normalized to unity) in the range of 0.5 to 0.9. This range of values compares favourably with more accurate spectroscopic values which follow from theoretical estimates, or extracted from proton knockout with electrons, both of which predict a number between 0.6 and 0.7.

The yield from the $(p, 2p)$ reaction for a heavy nucleus such as ^{197}Au or ^{208}Pb is only 3 to 5% of the plane wave prediction. Conversely, this means that of the order of 95% of the initial colliding nucleons suffer further violent interactions in the target nucleus.

Another convenient way to study $(p, 2p)$ knockout data is to display it as a function of binding energy. Results from Ref. [9] are shown in Figure 4. Knockout from various shell-model orbitals are clearly displayed, and again the DWIA theory gives an excellent reproduction of the data.

Not surprisingly, the experimental kinematic conditions, such as emission energies and scattering angles, have been carefully chosen in the examples of

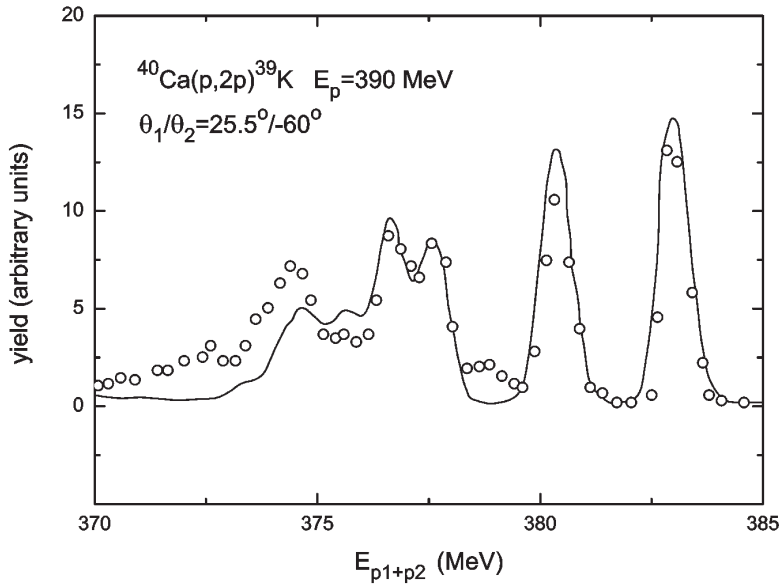


Figure 4. Binding energy distribution (sum of kinetic energies of the two outgoing protons) for the reaction $^{40}\text{Ca}(p,2p)^{39}\text{K}$ at an incident energy of 390 MeV and coplanar scattering angles on opposite sides of the incident beam as listed in the figure. The curves represent results of DWIA calculations, folded with the experimental binding energy resolution. Results are from Ref. [9].

$(p, 2p)$ reactions presented here to favour the knockout process. Nevertheless, a considerable attenuation of the initial knockout flux is implied by the extracted value of the spectroscopic factor. In the next section the question is addressed of what happens to the lost flux, and whether this can be observed experimentally and assessed theoretically.

4 Rescattering Following an Initial NN Interaction

In this section we explore the distribution of coincident protons induced by proton projectiles. However, whereas in $(p,2p)$ knockout measurements we chose scattering angles and emission energies optimized for such a process, we now explore a very different kinematic range. In order to select at least one emitted proton corresponding to the original NN interaction, we measure the particle p' in the $(p, p'p'')$ reaction at a relatively small scattering angle, and at a relatively high kinetic energy. In coincidence with this carefully selected particle p' we explore the emission-energy distribution of p'' . This should then reveal further energy-loss processes suffered by p'' subsequent to the NN collision.

In terms of a theoretical formulation [7], the cross section can be expressed as

$$\sigma = \sum_N \left[\int d\Omega_b \sum_\lambda \frac{d^3\sigma(\Omega_b, E_b)}{d\Omega_a d\Omega_b dE_a} \frac{1}{\sigma_N(E_b)} \frac{d^2\sigma(E_b, E_c)}{d(\Omega_c - \Omega_b) dE_c} \right], \quad (1)$$

in which, following Ref. [7], for clarity of notation the $(p, p'p'')$ reaction is rewritten as $A(p, ac)B$. The initial collision takes place between the projectile p and a bound nucleon b . Further rescattering of the b with the remainder of the target yields an observed particle c . Classically particle a corresponds to the scattered projectile. The quantities Ω and E are solid angles and kinetic energies of the particles denoted in the subscripts. The symbol N represents the type of bound nucleon b (either a proton or a neutron) participating in the initial collision that is associated with a specific shell model orbital λ . The quantity σ_N is the total cross section for the (b, c) reaction, which occurs as part of the subsequent intranuclear interaction.

As pointed out in Ref. [7], the triple differential cross section is related to the knockout reaction, but without inclusion of distortion in the wave function of the particle labelled b . Of course, this distortion is already included in the expression for the double differential cross section.

The structure of Eq. 1 reveals that it is related to the multistep formulation of the FKK theory. However, it only addresses two steps, namely the first step which is a collision which could in principle lead to knockout (represented by the triple differential cross section), and then a further interaction of the struck

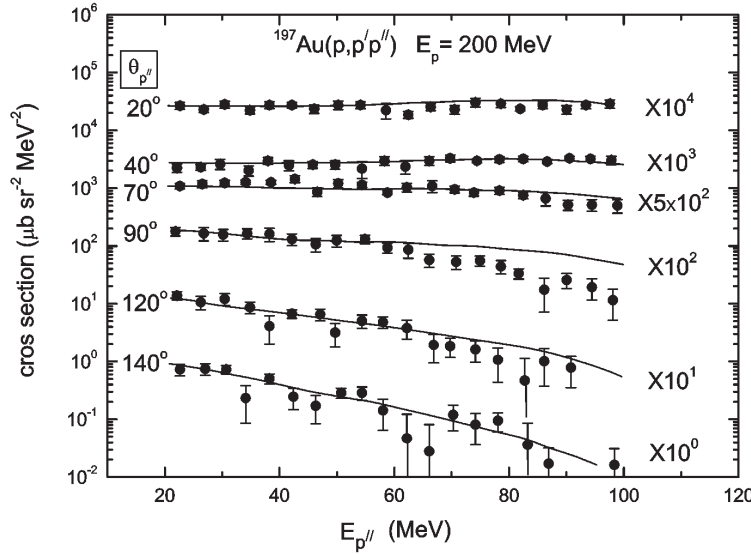


Figure 5. Cross sections for the $^{197}\text{Au}(p, p'p'')$ reaction at an incident energy of 200 MeV. Distributions are shown for a primary proton energy of $E_{p'} = 70$ MeV at a scattering angle of $\theta_{p'} = -40^\circ$. Secondary angles $\theta_{p''}$ are indicated in the figure. The curves represent results of calculations as described by Eq. 1. Results are from Ref. [7].

nucleon with the remainder of the target nucleus (represented by the double differential cross section). Of course, care should be taken to compare this theory in an experiment in which the kinematic condition of the primary proton is chosen to avoid further violent interactions with the target nucleus. This condition is achieved by selecting for the primary proton a scattering angle which is far forward, and by choosing a kinetic energy which is high compared to the incident energy. Under these conditions we explore the energy and spatial distribution of the secondary (struck in the first collision) protons. This is shown in Figure 5, together with the energy distributions predicted for various scattering angles. The experimental cross section increases as a function of secondary emission energy at forward angles, and at extreme backward scattering angles it drops off by almost two orders of magnitude from the lowest to the highest emission energy. Clearly the theory reproduces the experimental data remarkably well.

5 Reconstruction of an Inclusive Pre-Equilibrium Spectrum from Coincidence Information

The insight gained from knockout and rescattering coincidence experiments should enable one to reconstruct an inclusive pre-equilibrium spectrum for a forward scattering angle. A comparison from Ref. [10] between a theoretical prediction and an experimental inclusive energy distribution is reproduced in Figure 6. The agreement between theoretical and experimental distributions is satisfactory towards higher emission energies. However, at low emission ener-

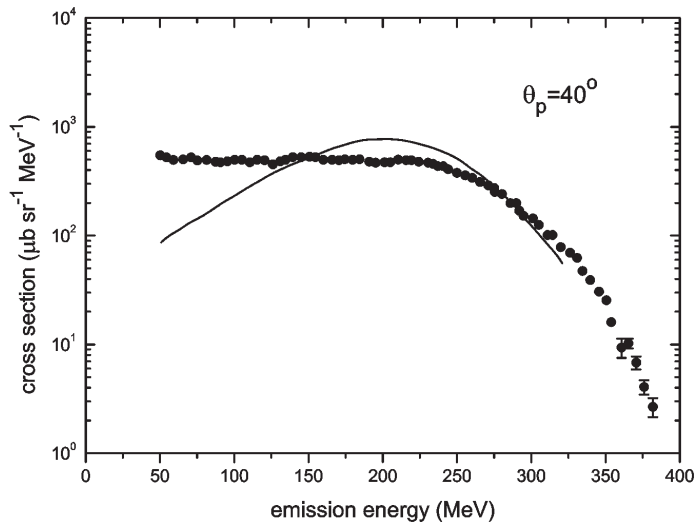


Figure 6. Comparison between an experimental inclusive pre-equilibrium spectrum for the $^{40}\text{Ca}(p, p')$ reaction at an incident energy of 390 MeV and a theoretical reconstruction based on coincidence studies as described in the text. Results are from Ref. [10].

gies the conditions for a favourable comparison is not satisfied, therefore the observed breakdown towards the low emission-energy region is not unexpected.

6 Summary and Conclusion

We find that the multistep interpretation as embodied in a number of theories which predict the dominant reaction mechanism leading to inclusive proton-induced reactions can be explicitly studied in knockout reactions, as well as coincident NN investigations. A consistent interpretation of several types of experimental studies is revealed, pointing to the general validity of the theoretical ideas.

Acknowledgement

This work was performed with funding from the South African National Research Foundation (NRF). The financial support is gratefully acknowledged.

References

- [1] E. Gadioli and P. E. Hodgson, *Pre-Equilibrium Nuclear Reactions* (Oxford University Press, New York, 1991).
- [2] A. J. Koning and J. M. Akkermans, *Phys. Rev. C* **47** (1991) 724–741.
- [3] H. Feshbach, A. Kerman and S. Koonin, *Ann. Phys. (NY)* 125 (1980)429.
- [4] A. A. Cowley, A. van Kent, J. J. Lawrie, S. V. Förtsch, D. M. Whittal, J. V. Pilcher, F. D. Smit, W. A. Richter, R. Lindsay, I. J. van Heerden, R. Bonetti, and P. E. Hodgson, *Phys. Rev. C* **43** (1991) 678–686.
- [5] N. S. Chant and P. G. Roos, *Phys. Rev. C* **15** (1977)57-68.
- [6] N. S. Chant and P. G. Roos, *Phys. Rev. C* **27** (1983) 1060–1072.
- [7] S. V. Förtsch, A. A. Cowley, J. J. Lawrie, J. V. Pilcher, F. D. Smit, and D. M. Whittal, *Phys. Rev. C* **48** (1993) 743– 755.
- [8] R. Neveling, A. A. Cowley, G. F. Steyn, S. V. Förtsch, G. C. Hillhouse, J. Mano, and S. M. Wyngaardt, *Phys. Rev. C* **66** (2002) 034602.
- [9] A. A. Cowley, G. J. Arendse, R. F. Visser, G. F. Steyn, S. V. Förtsch, J. J. Lawrie, J. V. Pilcher, T. Noro, T. Baba, K. Hatanaka, M. Kawabata, N. Matsuoka, Y. Mizuno, M. Nomachi, K. Takahisa, K. Tamura, Y. Yuasa, H. Sakaguchi, T. Itoh, H. Takeda, and Y. Watanabe, *Phys. Rev. C* **57** (1998) 3185–3190.
- [10] A. A. Cowley, G. F. Steyn, Y. Watanabe, T. Noro, K. Tamura, M. Kawabata, K. Hatanaka, H. Sakaguchi, H. Takeda, and M. Itoh. *Phys. Rev. C* **62** (2000) 064604.